Robust Real-Time UAV Based Power Line Detection and Tracking

Guang Zhou, Jinwei Yuan, I-Ling Yen, Farokh Bastani
Department of Computer Science
University of Texas at Dallas, Richardson, Texas, USA
{gxz110430, jxy123730, ilyen, bastani}@utdallas.edu

Abstract. Power line inspection is an essential but costly task while automated UAV (unmanned aerial vehicle) inspection can greatly reduce such costs. However, navigating along power lines is a challenging task due to the narrow width and limited features of power lines. Existing power line tracking methods have threshold selection problems and cannot work well for complex and changing backgrounds. We make use of power line specific knowledge to build a model to achieve predictive and continuous parameter selection so that the best thresholds are selected for changing scenarios. Experimental studies show that our solution is much better than existing ones. Specifically, we have built the first fully automated UAV that successfully tracks power lines in the real world.

Keywords. UAV, Power line inspection, Object tracking, Hough transformation.

1 Introduction

Overhead high-voltage power transmission lines are vital elements of modern industry and urban life [1]. The components in the power delivery infrastructure, such as conductor cables, transformers, splices, insulators, etc., may incur wear and tear and other damages, causing problems in electricity delivery or even dangerous consequences. Power companies spend a lot of money and efforts to perform regular inspections and maintenance to ensure the reliability of these components. In this paper, we consider the inspection of power lines and the splices and insulators on these lines. Power line inspection methods used in practice and proposed in the literature include ground patrol, helicopter, rolling robots, and UAVs. Inspection of high-voltage power lines can be very dangerous if performed by humans and very expensive if performed by helicopters. The rolling robot solution [2,3] requires robots to be attached to the cable and, hence, can effectively inspect power lines at a close distance. But the weight of the robots could damage the cable and the robots may not be able to pass across various obstacles on the cable. UAV is, hence, the best instrument for detailed power line inspection tasks.

UAV assisted power line inspection is still an emerging technology and there are only a few developers worldwide. In earlier works, the UAV was controlled by humans and the collected data are analyzed offline [4]. Over the past decade, various power line tracking methods have been proposed, including pole detection based [5], GPS way points based [6], and power line detection based [7,8,9,10]. Pole detection based navigation detects electricity poles without providing specific methods for navigating along the power lines. Thus, they are not suitable for power line inspection. The Japanese companies Hirobo and Chugoku [6] have developed a navigation system based on the GPS waypoints obtained through pre-specified locations of electricity poles. This method requires the availability of the electricity network map. Also, GPS has error range that is beyond the required navigation accuracy for power line inspection. Thus, the navigation decision still requires power line detection.

The power line detection based navigation approach detects power lines from the images taken by the UAV during its flight and uses the detected power lines to guide its navigation closely along the power lines. If done properly and in real time, it can be the most effective navigation solution for power line inspection tasks. However, existing object detection/tracking methods cannot be applied to power line detection directly since power lines are very thin and lack rich features. Also, methods specifically designed for power line detection [7,8,9,10] do not perform well in the real world. Generally, power line detection consists of edge detection and Hough transformation steps. In traditional power line tracking solutions, a threshold is set manually for its edge detection algorithms [7,8,9]. However, a fixed threshold may cause these algorithms to fail with complex and changing backgrounds. Methods in [7,8,9] are only effective when the background is relatively monotonic. In [10], PCNN (pulse coupled neural network) filter is used to remove the noise during edge detection. The number of iterations defined in the PCNN filter has a similar role as a threshold and, hence, it incurs the same threshold selection problem as other methods. The second problem in existing methods is the way they capture power line images, in which the cameras are set to look vertically down to the ground, resulting in limited viewing range and subsequently poor tracking, especially when there are sudden changes in the background.

In this paper, we first propose a novel method that can effectively tune the thresholds in detection algorithms. We observe that the high level spatial information of the power lines is very helpful to filter out noise for edge detection. Accordingly, we introduce a parameter mapping method to associate the optimal detection parameters with the corresponding backgrounds. In each frame, a power line model is built and saved. For the unvisited background, the UAV uses the power line model detected in previous frames to select the best parameters. For the visited background, the optimal parameters are reused. By doing so, the accuracy of the edge detector is improved since the parameters used for the corresponding background is always optimal. For the second problem, we tilt the camera to face the power line at an angle so that a larger region of the power line can be shown in the frame. By doing so, each input frame provides a globalized view of where the power line goes and, hence,

benefits power line tracking.

In the experiment study, we have implemented our algorithm on a real UAV platform which is equipped with a high definition gyro stabilized camera. Experimental results show that our approach significantly outperforms other existing approaches. Also, most existing methods are studied in an offline manner. They experiment on manually recorded videos that are not the same as the real images captured by an inspecting UAV. To the best of our knowledge, our system is the first fully automated UAV which tracks power lines under different backgrounds and varying luminations in real environment at speeds up to 30km/h. It has won the first prize in the 2nd DJI developer challenge competition [11].

2 Preliminaries

Power Line Model. We use some characteristics of the overhead power lines to assist the power line detection and tracking by UAVs. Below are some observations that can help construct the power line model from 2D camera images:

1. Power lines are straight lines when viewed from above. They may sag vertically due to the gravity, which is generally not captured by the top view camera. They only change directions when some poles exist. The pole is approximately the angular bisector of the power lines. In Figure 1a, the difference between the angle is bounded by a value $\delta = |\alpha - \beta|$, which typically is less than 10 degrees.
2. Power lines are normally brighter than the background because the specific metal used has a higher reflection rate.
3. Power lines are approximately parallel to each other and their intersecting angle in an image is generally very small (e.g. 3 degrees). For simplicity, we assume that all these parallel power lines are exactly the same as each other, but with a shift at a distance D_{ij} between power lines *i* and *j*.

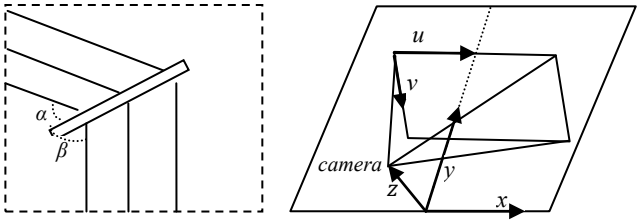

Figure 1. (a) Pole model. (b) *W* and *I* spaces.

Image Model. A camera image captures a 3D physical space into a 2D discrete image space. Let $I = \{(u, x)\} \in N^2$ represent the 2D discrete image space and $W = \{(x, y, z)\} \in R^3$ represents the continuous 3D physical space captured by I. Figure 1b shows the relationship between I and W. In order to get the mapping from I space to W space, the following parameters need to be known:

- 2α : The camera field of view.
- f: The focus length of the lens.
- $n \times n$: The resolution of camera.
- (x_c, y_c, z_c): The coordinates of the camera view point in the W space, which is obtained from GPS coordinates. Note that the GPS accuracy of the drone is vertical 0.5m and horizontal 1.5m which is sufficiently accurate for our power line detection algorithm.
- θ: Camera viewing angle (the angle between the optical axle of the camera and the horizontal plane, which is given by the IMU data).
- γ: Camera heading angle (the angle between the projection of the optical axle on the plane $z = 0$ and the y axle, which is the same as the compass data).

We can map any point (u, v) in the image space I to the point (x, y, z) in the physical space W as follows [12].

$$x(u,v) = z_c \times ctg\left[\theta - \alpha + \frac{2v\alpha}{n-1}\right] \times sin\left[\gamma - \alpha + \frac{2u\alpha}{n-1}\right] + x_c$$
$$y(u,v) = z_c \times ctg\left[\theta - \alpha + \frac{2v\alpha}{n-1}\right] \times cos\left[\gamma - \alpha + \frac{2u\alpha}{n-1}\right] + y_c$$
$$z(u,v) = 0 \qquad (1)$$

3 Power Line Tracking Algorithm

Figure 2 shows the basic flow for our tracking algorithm. Our image processing starts by cutting the input image by sliding the line model from the previous frame. The Region of Interest (RoI) is selected to further analyze and track the power lines. Proper RoI identification can reduce the search space in later phases. For the initial frame, we assume that the power line model is given by the user..

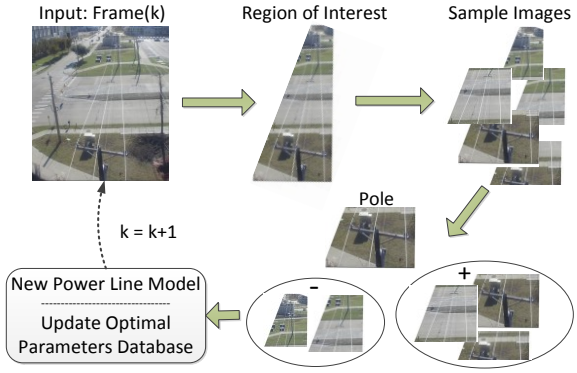

Figure 2 Overall flow of the detection algorithm

In the next step, a set of n patches $\{P_1, P_2, \ldots \ldots P_n\}$ are cropped from the RoI for further processing.

$$P_i = \{(u,v) | (u,v) \in ROI, l_1 \leq v \leq l_2\} \qquad (2)$$

where l_1, l_2 are two lines described by $v = l_1$, $v = l_2$. Then, existing object (pole) detection algorithms, such as those given in [5][13], will be applied on all patches. For any pole that is found, its direction information will be extracted.

Next we improve the edge detection kernel (discussed in Section 3.2) and hysteresis thresholding (discussed in Section 3.3) in Canny's approach. In the aero captured image, the optimal edge detection parameters for the same background are almost the same when viewing from different directions. Based on this observation, we assume

that the optimal parameter is a function of the coordinates (x, y, z) in the *W* space. We then map each point in an image to the corresponding physical space (mapping function is given in Section 3.1). Via this mapping, the UAV can obtain the associated coordinates for all patches. As the UAV is flying, an optimal parameter database is built and saved. For each incoming image, a patch is categorized as positive if its associated GPS coordinates are found in the database; otherwise, it is categorized as negative. For the positive patches, the optimal parameters in the database are used for edge detection. For the negative patches, the optimal parameters are predicted based on the power line model and then stored into the database.

Next, a constrained Hough Transform is used to filter the irrelevant linear structures (Section 3.4). Then, the new power line model is reconstructed based on the power lines and poles detected in all the patches. Finally, we move to the next frame.

3.1 Power Line Image Mapping

In Section 2, we assumed that the power lines are approximately straight lines and parallel to each other. However, in *I* space, all power lines are converged to a single point, called vanished point (VP). The function for all possible power lines is expressed by Equation 3:

$$v - v_p = m(u - u_p) \tag{3}$$

where (u_p, v_p) is the coordinate for the VP at *I* space and *m*, $(-\infty, \infty)$, is the slope of the lines.

Also, we assumed that the power line is a shifted version of other power lines at a distance $D_{ij} = (x_i - x_j)$, where x_i is the coordinate of *i*'th power line on the *x* axis in *W* space. Hence, in *I* space, the horizontal distance $d_{ij} = (u_i - u_j)$ between points $p(u_i, v)$ and $p(u_j, v)$ is:

$$d_{ij} = \frac{D_{ij} f^2 (v - v_p)}{z_c (f^2 + {v_p}^2)} \tag{4}$$

where *f* is the focus length of the lens and $p(u_i, v)$ and $p(u_j, v)$ are points projected from power lines. Based on Equations (3,4), we are able to design our edge detector and line detector in the following subsections.

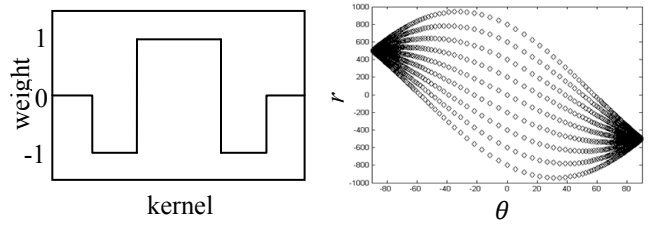

Figure 3 (a)One dimension kernel (b)Constrained Hough Space

3.2 Edge Detector Kernel Design

The operators used in general edge detection methods [7,8,9,10] enhance both linear objects (e.g. power lines) and the edge of strong contrasting areas which could have negative impacts on the power line detection. We design a one dimensional kernel to replace the Sobel kernel in Canny edge detection and the shape of the kernel is shown in Figure 3a. In *I* space, the power lines have varying thicknesses across the image. By substituting *d* (the diameter of the power line cable) into Equation 4, the thickness of power line in *I* space is as follow:

$$d(v) = \frac{(v - v_p)}{(n - v_p)} d_{bottom}, where\ d_{bottom} = \frac{d f^2 (n - v_p)}{z_c (f^2 + {v_p}^2)} \tag{5}$$

Note that d_{bottom} (typically 10 pixels) is the thickness at the bottom. Based on Equation 5, the width of the kernel is determined only by the *v* coordinate in *I* space. By convolving the kernel in both vertical and horizontal dimensions, we get the edge strength in both directions.

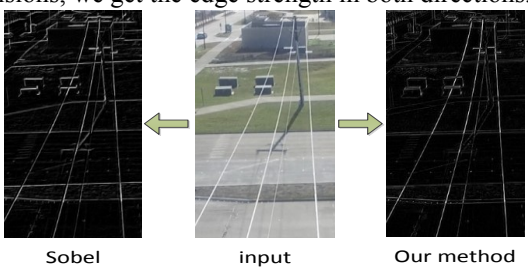

Figure 4. Result of one dimension kernel

Figure 4 shows that our varying length kernel discards most of the clutters (dark linear objects and edges between strong contrasting areas) and has a strong response only to bright linear features.

3.3 Parameter Prediction for Edge Detection

After deriving the intensity gradient of the image, we perform common edge thinning (same as Canny's). Then, we developed a prediction based method for selecting the two thresholds in the hysteresis thresholding step by making use of the power line model (as shown in Figure 5).

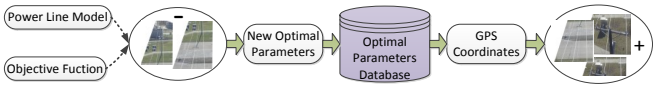

Figure 5. Parameter Prediction Diagram

For each incoming patch P_i described by Equation 2, its corresponding area S_i in *W* space is as follows:

$$S_i = \{(x(u,v), y(u,v), z(u,v)) | (u,v) \in P_i\} \tag{6}$$

where the mapping functions $x(u,v), y(u,v), z(u,v)$ have been given in Equation 1.

In our method, the UAV keeps an optimal parameter database for the visited places. For the positives patches, UAV will retrieve its optimal parameters based on its associated GPS coordinates. For the negative patches, we use an objective function and power line model to predict the best parameters. Before giving the objective function, we first classify an edge pixel *e* as a signal pixel if it satisfies Inequality 7, otherwise it is classified as a noise pixel.

$$\min_{l \in L} \{dis(e,l)\} \leq mindis \tag{7}$$

where *L* is the power lines set detected by the previous frame. Function $dis(e,l)$ returns the distance between edge pixel *e* and power line l. *mindis* is the minimum distance we consider a pixel as a signal pixel. Finally, we give the

objective function as follows:

$$f\big(E(P_i,\vec{p})\big) = \frac{number\ of\ signal\ pixels\ in\ E}{number\ of\ noise\ pixels\ in\ E} \quad (8)$$

where $E(P_i,\vec{p})$ is the edge map of patch P_i and $\vec{p}$ is its detection parameter.

The objective function calculates the signal to noise ratio of the edge image. Subsequently, the optimal parameter $\vec{p}_{optimal}$ can be found by maximizing f in Equation 8:

$$\vec{p}_{optimal} = argmin_{\vec{p}} f\big(E(P_i,\vec{p})\big) \quad (9)$$

3.4 Constrained Hough Line Detection

Hough transform is used to detect lines by mapping all edge pixels into a parameter space. The lines are detected by choosing the peaks in the space. Hough transform is powerful in line detection, but it cannot intelligently identify power lines from other linear structures. In order to solve this problem, we again use the high level spatial information of the power lines to filter the irrelevant linear structures.

A straight line $y = ax + b$ can be expressed as (r,θ) in parameter space, where r is the distance from the origin to the closest point on the line and θ is the angle between the x axis and the line. By substituting into Equation 3, we have Equation 10 which describes (r,θ) for all lines that share the same VP (u_p, v_p) as follows:

$$r = \frac{m * u_p - v_p}{\sqrt[2]{1+m^2}} \quad \text{and} \quad \theta = \tan^{-1} m \quad (10)$$

The curves in Figure 3b show all possible peaks for different VPs in the parameter space. In our constrained Hough line detection, we only search the space which is near the curve. This method has been proven to work in our experiments since the difference for the same power lines detected in continuous frames is very small.

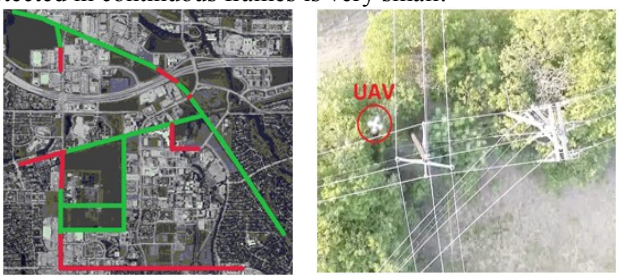

Figure 6 (a) Testing environment (b) Failure case analysis

4 Experimental Results

Unlike other works, we tested our algorithm in a large scale real world environment. A UAV (DJI Phantom III), equipped with 94° field of view camera, is used. The computation is done by an iPad Air 2 with A8X chip. Figure 6a shows the aerial map of our testing environment. The autonomously tracked power lines are marked as green in areas where the environment is relatively simple, and red in areas where the environment is complex with a lot of artificial structures. The UAV cruising speed is set to 30 km/hour in green lines and 15km/hour in red lines.

Due to the benefit of the power line model and the improved mapping/prediction scheme, our algorithm outperforms all of the traditional power line detection methods, especially in complex backgrounds (red line area). Figure 7 shows the comparison results. The original image at Row 1a shows one of the scenarios of complex backgrounds. The images at Row 1b and Row 2 are the results of Hough transform on Canny and our edge map. The images at Row 1c and Row 3 are the results of Constrained Hough transform on Canny and our edge maps. From the results, it clearly shows that our method (Row 1b/c) archives better performance than the manually tuned best Canny and Hough transform results (Row 2/3). With the same parameters, our improved edge detection kernel (Row 1c) outperforms Sobel kernel (Row 3b).

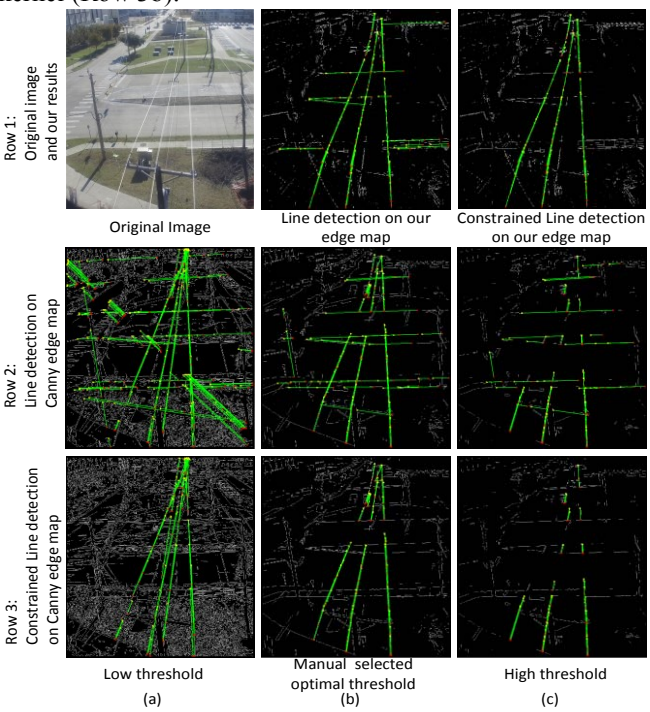

Figure 7. Results comparison

Image from another UAV at typical failure cases is shown in Figure 6b. The location of the UAV is marked in red. The common causes for the failures are the other poles which belong to different power line sets that are captured by the camera. Our method does not handle such intersections very well. The UAV randomly chooses one of the power lines instead of following the original one.

5 Conclusion

We propose a novel edge detection method, which selects optimal parameters for changing backgrounds, and, hence, overcomes the threshold problem in existing methods. Also, our method requires relatively low computation recourses when compared to existing methods. Our system achieved the fully automated power line tracking in Dallas, Texas, through a 15 km power lines with speeds up to 30km/h. It is a robust real time power line tracking method in real world.

6 Reference

[1] The Great Soviet Encyclopedia, 3rd Edition (1970-1979).

[2] Mostashfi, A., A. Fakhari, and Mohammad Ali Badri. "A novel design of inspection robot for high-voltage power lines." Industrial Robot: An International Journal 41, no. 2 (2014): 166-175.

[3] Pouliot, Nicolas, and Serge Montambault. "Geometric design of the LineScout, a teleoperated robot for power line inspection and maintenance." In Robotics and Automation, 2008. ICRA 2008. IEEE International Conference on, pp. 3970-3977. IEEE, 2008.

[4] Ishino, R., and F. Tsutsumi. "Detection system of damaged cables using video obtained from an aerial inspection of transmission lines." In Power Engineering Society General Meeting, 2004. IEEE, pp. 1857-1862. IEEE, 2004.

[5] Golightly, Ian, and Dewi Jones. "Corner detection and matching for visual tracking during power line inspection." Image and Vision Computing 21, no. 9 (2003): 827-840.

[6] http://www.energia.co.jp/e/

[7] Golightly, Ian, and Dewi Jones. "Visual control of an unmanned aerial vehicle for power line inspection." In Advanced Robotics, 2005. ICAR'05. Proceedings., 12th International Conference on, pp. 288-295. IEEE, 2005.

[8] Jones, Dewi, Ian Golightly, Jonathan Roberts, and Kane Usher. "Modeling and control of a robotic power line inspection vehicle." In Computer Aided Control System Design, 2006 IEEE International Conference on Control Applications, 2006 IEEE International Symposium on Intelligent Control, 2006 IEEE, pp. 632-637. IEEE, 2006.

[9] Zhang, Jingjing, Liang Liu, Binhai Wang, Xiguang Chen, Qian Wang, and Tianru Zheng. "High speed automatic power line detection and tracking for a UAV-based inspection." In Industrial Control and Electronics Engineering (ICICEE), 2012 International Conference on, pp. 266-269. IEEE, 2012.

[10] Li, Zhengrong, Yuee Liu, Ross Hayward, Jinglan Zhang, and Jinhai Cai. "Knowledge-based power line detection for UAV surveillance and inspection systems." In Image and Vision Computing New Zealand, 2008. IVCNZ 2008. 23rd International Conference, pp. 1-6. IEEE, 2008.

[11] https://www.dji.com/info/news/report-from-the-2nd-dji-developer-challenge

[12] Bertozzi, Massimo, and Alberto Broggi. "GOLD: A parallel real-time stereo vision system for generic obstacle and lane detection." Image Processing, IEEE Transactions on 7, no. 1 (1998): 62-81.

[13] Viola, Paul, and Michael Jones. "Rapid object detection using a boosted cascade of simple features." In Computer Vision and Pattern Recognition, 2001. CVPR 2001. Proceedings of the 2001 IEEE Computer Society Conference on, vol. 1, pp. I-511. IEEE, 2001.